VOLUME 70, NUMBER 23

JOC Articles

NOVEMBER 11, 2005

DNA Cleavage by the Photolysis of Cyclopentadienyl Metal Complexes: Mechanistic Studies and Sequence Selectivity of Strand Scission by $CpW(CO)_3CH_3$

Debra L. Mohler,*[,†,||] Jennifer R. Downs,[†] Allison L. Hurley-Predecki,[†] Jennifer R. Sallman,[†] Peter M. Gannett,*[,‡] and Xianglin Shi[§]

Department of Chemistry, Emory University, 1515 Dickey Drive, Atlanta, Georgia 30322, Department of Basic Pharmaceutical Sciences, West Virginia University, P.O. Box 9530, Morgantown, West Virginia 26506-9530, and Health Effects Laboratory Division, National Institute for Occupational Safety and Health, Morgantown, West Virginia 26505

dmohler@emory.edu

Received February 22, 2005

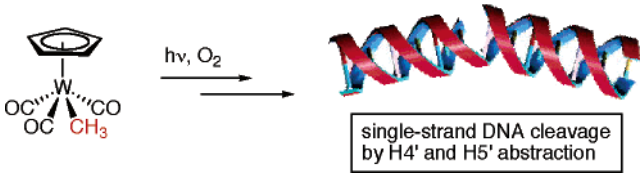

The photolysis of $CpW(CO)_3Me$ has been shown to produce methyl radicals and to cleave DNA in a single-stranded manner, and preliminary evidence implicated a carbon-centered radical in this process. In this work, the mechanism of strand scission in this reaction was determined to occur by hydrogen atom abstraction from the 4′- and 5′-positions of the deoxyribose moiety of the backbone of DNA. Additionally, in a side reaction that does not lead to frank strand scission, all four bases of DNA are methylated under these conditions; however, none of these base or backbone modifications lead to the formation of abasic sites.

Introduction

Hydroxyl radical has shown great utility in vitro as a tool for the elucidation of the structure of DNA[1] and of the DNA-binding sites of proteins[2] and small molecules.[3] While the generation of hydroxyl radical in such studies is accomplished most commonly by the reaction of Fe(II)·EDTA with hydrogen peroxide, applications in vivo require other sources, including γ[4] or synchotron X-ray irradiation.[5] Although not always readily available, these latter methods possess the advantageous ability to provide time-resolved data and thus information about the dynamic processes of such biomacromolecules.

While the field of hydroxyl radical-mediated DNA damage was initiated in part by findings related to the biological effects of γ-radiolysis,[6] the study of DNA cleavage by carbon-centered radicals began with the discovery of the biological activity of the enediyne antitumor antibiotics.[7] These natural products evolved for

† Emory University.
‡ West Virginia University.
§ National Institute for Occupational Safety and Health.
|| Present address: James Madison University, Harrisonburg, VA. Tel: 540-568-8803. Fax: 540-568-7938. E-mail: mohlerdl@jmv.edu.

(1) For lead references see: Tullius, T. D. In *Radiation Research*; Moriarty, M., Ed.; Allen Press: Lawrence, KS, 2000; Vol. 2, pp 333−335.
(2) For example: Frazee, R. W.; Taylor, J. A.; Tullius, T. D. *J. Mol. Biol.* **2002**, *323*, 665−683.
(3) Trauger, J. W.; Dervan, P. B. *Methods Enzymol.* **2001**, *340*, 450−466.
(4) For example: Ottinger, L. M.; Tullius, T. D. *J. Am. Chem. Soc.* **2000**, *122*, 5901−5902.
(5) For example: Brenowitz, M.; Chance, M. R.; Dhavan, G.; Takamoto, K. *Curr. Opin. Struct. Biol.* **2002**, *12*, 648−653.
(6) von Sonntag, C. *The Chemical Basis of Radiation Biology*; Taylor and Francis: London, UK, 1987.
(7) For lead references see: Smith, A. L.; Nicolaou, K. C. *J. Med. Chem.* **1996**, *39*, 2103-2117.

10.1021/jo050338h CCC: $30.25
Published on Web 05/17/2005

selective strand scission in vivo to incorporate recognition elements and triggering devices that prevent premature production of the active carbon-centered radical species. Because of the significant synthetic challenge posed by these complex molecules, numerous analogues[8] and precursors to simple organic radicals have been examined for their ability to alkylate DNA bases,[9−14] in addition to causing strand scission[15,16] by abstracting hydrogen atoms from the sugar−phosphate backbone of DNA, although not all of these compounds are suitable for footprinting use in vivo. Therefore, in the search for a reagent that combines the availability of the Fe(II)·EDTA/H_2O_2 system with a unimolecular triggering device and in vivo capability, we recently reported the photoinduced cleavage of DNA by complexes of the general formula $CpM(CO)_nR$, in which M is Fe (n = 2) or W (n = 3) and R is CH_3 or C_6H_5.[17]

The above complexes were chosen because each can be prepared easily by literature methods and is stable to the aqueous aerobic conditions required for DNA cleavage experiments. Additionally, these molecules offer a potentially diverse array of reactivities through tuning of the ligand sphere; and their many spectroscopic characteristics allow one to monitor their reactions and binding to DNA. Their Cp ligands are tightly bound,[18] providing a location to attach biomolecular recognition elements without perturbing the reactivity of the metal center. Most importantly, for each complex, there was some reported evidence for the desired photochemical production of either methyl or phenyl radicals (Scheme 1),[19,20] both of which had been shown to cleave DNA.

It is generally accepted that the primary photoprocess for complexes **1**−**4**, in which M = W (n = 3) or Fe (n = 2) and R = CH_3 or C_6H_5, involves loss of carbon monoxide (to give **6**), which may be accompanied by homolysis of the metal−methyl or metal−aryl bond to yield the metal-based radical **5** along with methyl or phenyl radical. However, radical formation may occur by multiple pathways, as has been suggested for the photolysis of $CpW(CO)_3CH_3$ (**1**), the complex whose photochemistry has been most extensively studied.[21−23] In this case, it has been proposed that $CpW(CO)_2CH_3$ (**6**, in which M = W) reacts with another molecule of starting material to produce the metal−metal bonded species **7** and two methyl radicals. Furthermore, it has been demonstrated that the 16 electron species $CpW(CO)_2CH_3$ (**6**) can coordinate a variety of ligands (e.g., L = PR_3, CH_3CN, THF, or H_2O);[24,25] and when $CpW(CO)_2(PPh_3)CH_3$ (either purified or produced in situ during the photolysis of **1** in the presence of PPh_3) is photolyzed, methyl radicals are formed.[22]

SCHEME 1

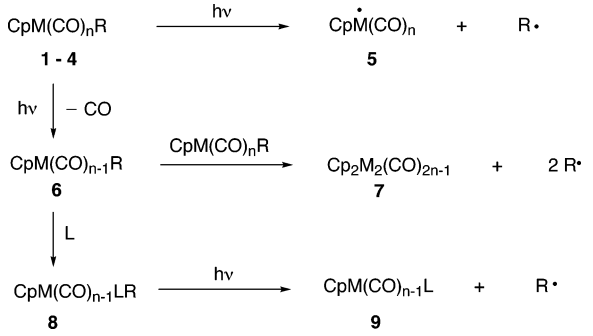

As a prerequisite for employing $CpM(CO)_nR$ complexes for footprinting DNA−protein assemblies and for studying small DNA-binding molecules via affinity cleavage, we have optimized the DNA cleaving behavior of substituted analogues of $CpW(CO)_3R$ (R = CH_3 (**1**) or C_6H_5 (**2**)) for nonrandom double-strand scission[26] and for sequence-selectivity.[27] The effect of the metal center has also been assessed, showing that the corresponding iron complexes $CpFe(CO)_2R$ (but not those containing chromium or molybdenum) are also efficient photocleaving agents.[17] In all cases, preliminary experiments implicated carbon-centered radicals as the active species, ultimately leading to DNA strand scission.[17,28] Here, we report the results of the more detailed investigation of the mechanism of strand scission by one of the parent complexes, $CpW(CO)_3CH_3$ (**1**).

Results

Plasmid DNA Cleavage and the Potential Role of Methyl Radical. The DNA-cleaving ability of complex

(8) Recent examples: Dai, W.-M. *Curr. Med. Chem.* **2003**, *10*, 2265−2283. Kovalenko, S. V.; Alabugin, I. V. *Chem. Commun.* **2005**, 1444−1446. Tuntiwechapikul, W.; David, W. M.; Kumar, D.; Salazar, M.; Kerwin, S. M. *Biochemistry* **2002**, *41*, 5283−5290. Suzuki, I.; Shigenaga, A.; Nemoto, H.; Shibuya, M. *Tetrahedron Lett.* **2004**, *45*, 1955−1959.

(9) Gannett, P. M.; Heavner, S.; Daft, J. R.; Shaughnessy, K. H.; Epperson, J. D.; Greenbaum, N. L. *Chem. Res. Toxicol.* **2003**, *16*, 1385−1394.

(10) Gannett, P. M.; Shi, X.; Ye, J.; Powell, J. H.; Darian, E.; Daft, J. R. *Chem. Res. Toxicol.* **2000**, *13*, 1020−1027.

(11) Gannett, P. M.; Powell, J. H.; Rao, R.; Shi, X.; Lawson, T.; Kolar, C.; Toth, B. *Chem. Res. Toxicol.* **1999**, *12*, 297−304.

(12) Gannett, P. M.; Lawson, T.; Miller, M.; Thakkar, D. D.; Lord, J. W.; Yau, W.-M.; Toth, B. *Chem.-Biol. Interact.* **1996**, *95*, 1−25.

(13) Netto, L. E. S.; RamaKrishna, N. V. S.; Kolar, C.; Cavalieri, E.; Rogan, E.; Lawson, T.; Augusto, O. I. *J. Biol. Chem.* **1992**, *267*, 21524−21527.

(14) Augusto, O.; Cavalieri, E. L.; Rogan, E. G.; RamaKrishna, N. V. S.; Kolar, C. *J. Biol. Chem.* **1990**, *265*, 22093−22096.

(15) For lead references see: Armitage, B. *Chem. Rev.* **1998**, *98*, 1171−1200. Shimakoshi, H.; Kaieda, T.; Matsuo, T.; Sato, H.; Hisaeda, Y. *Tetrahedron Lett.* **2003**, *44*, 5197−5199. Wender, P. A.; Touami, S. M.; Alayrac, C.; Philipp, U. C. *J. Am. Chem. Soc.* **1996**, *118*, 6522−6523. Arya, D. P.; Jebaratnam, D. J. *Tetrahedron Lett.* **1995**, *36*, 4369−4372.

(16) Riordan, C. G.; Wei, P. *J. Am. Chem. Soc.* **1994**, *116*, 2189−2190.

(17) Mohler, D. L.; Barnhardt, E. K.; Hurley, A. L. *J. Org. Chem.* **2002**, *67*, 4982−4984.

(18) Crabtree, R. H. *The Organometallic Chemistry of the Transition Metals*; Wiley: New York, 1994.

(19) Samuel, E.; Rausch, M. D.; Gismondi, T. E.; Mintz, E. A.; Giannotti, C. *J. Organomet. Chem.* **1979**, *172*, 309−315.

(20) Gismondi, T. E.; Rausch, M. D. *J. Organomet. Chem.* **1985**, *1985*, 59−71. Alt, H. G.; Herberhold, M.; Rausch, M. D.; Edwards, B. H. *Z. Naturforsch. B*: *Anorg. Chem., Org. Chem.* **1979**, *34B*, 1071−1077.

(21) Virrels, I. G.; George, M. W.; Johnson, F. P. A.; Turner, J. P.; Westwell, J. R. *Organometallics* **1995**, *14*, 5203−5208. Goldman, A. S.; Tyler, D. R. *Inorg. Chem.* **1986**, *25*, 706−708. Kazlauskas, R. J.; Wrighton, M. S. *J. Am. Chem. Soc.* **1982**, *104*, 6005−6015.

(22) Goldman, A. S.; Tyler, D. R. *J. Am. Chem. Soc.* **1986**, *108*, 89−94.

(23) Tyler, D. R. *Inorg. Chem.* **1981**, *20*, 2257−2261.

(24) Yang, G. K.; Peters, K. S.; Vaida, V. *J. Am. Chem. Soc.* **1986**, *108*, 2511−2513.

(25) Alt, H. G.; Schwarzle, J. A. *J. Organomet. Chem.* **1978**, *162*, 45−56. Severson, R. G.; Wojcicki, A. *J. Organomet. Chem.* **1978**, *157*, 173−185.

(26) Hurley, A. L.; Mohler, D. L. *Org. Lett.* **2000**, *2*, 2745−2748.

(27) Hurley, A. L.; Maddox, M. P. I.; Scott, T. L.; Flood, M. R.; Mohler, D. L. *Org. Lett.* **2001**, *3*, 2761−2764.

(28) Mohler, D. L.; Dain, D. R.; Kerekes, A. D.; Nadler, W. R.; Scott, T. L. *Bioorg. Med. Chem. Lett.* **1998**, *8*, 871−874.

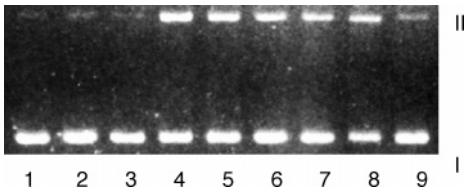

FIGURE 1. Photoinduced cleavage of pBR322 DNA (30 μM/bp in 10% DMSO/10 mM Tris buffer, pH 8) by $CpW(CO)_3CH_3$ (**1**): lane 1, DNA alone; lane 2, DNA alone, irradiated; lane 3, DNA + complex (720 μM), no irradiation; lanes 4 through 9, DNA + complex (720, 360, 180, 90, 45, and 23 μM, respectively). Reactions in lanes 4−9 were irradiated with Pyrex-filtered light from a 450-W medium-pressure mercury arc lamp for 20 min.

SCHEME 2

$$\underset{\mathbf{1}}{CpW(CO)_3CH_3} \xrightarrow{h\nu,\ THF\text{-}d_8} [CpW(CO)_3]_2 + CH_4 + CH_3D$$

1 was demonstrated initially by a plasmid relaxation assay, in which the conversion of circular supercoiled DNA (form I) to relaxed circular (form II) or linear (form III) DNA was monitored. Thus, various concentrations of **1** were irradiated in the presence of pBR322 DNA (Figure 1), giving single-strand cleavage. Control experiments showed that both light and **1** were required to effect strand scission (lanes 2 and 3), which occurred in a concentration-dependent manner (lanes 4−9) at ratios above 1.5 molecules/base pair. This value was surprisingly low considering that the complex lacks a DNA binding element and that most synthetic enediynes (which generate diradicals) without recognition devices require 100−1000 molecules/base pair to exert this behavior. The use of other organic solvents (EtOH, dioxane, THF) to solubilize the complex gave cleavage at similar molecule/base pair ratios as DMSO.[29]

On the basis of the hypothesis that the photogenerated methyl radical initiates DNA cleavage, its hydrogen atom abstraction ability was examined by conducting the photolysis of **1** (3.3 M) in THF-d_8 in the presence of air (Scheme 2). The deuterated THF was used to model the sugar portion of the DNA backbone, since similar experiments with DNA would require deuterated DNA and because the concentrations at which the DNA cleavage experiments are conducted are typically too low to allow for the unambiguous detection of the methyl radical-derived products. Preliminary results indicated that the prevailing methyl radical-derived products detected by GC-MS were methane-d_1 and methane (in approximately a 1:2 ratio), a result that is in accord with the production of methyl radical followed by deuterium or hydrogen atom abstraction from THF-d_8 or a metal complex,[30] respectively. In comparison, a control experiment conducted in nondeuterated THF showed only negligible amounts of a species with an *m/z* of 17. In neither case were any products derived from methylperoxyl radical (the product of the reaction of methyl radical with dioxygen) observed, but the likelihood that any such products would survive GC-MS is very low. Since the production of nondeuterated methane can be attributed to a cage effect, the detection of CH_3D suggested that methyl radical is capable of abstracting hydrogens from the sugar−phosphate backbone of DNA. Although abstraction from a metal complex competes with that from THF-d_8 in this simple photolysis experiment, such a cage effect apparently does not prevent DNA cleavage (vide infra) when the radical is produced in the highly structured environment of DNA.

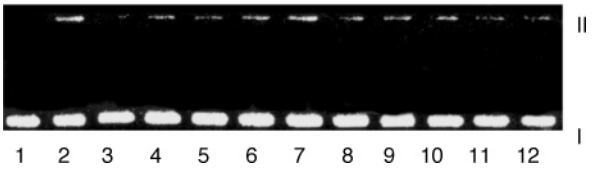

FIGURE 2. Inhibition by cysteine and TEMPO of cleavage of pBR322 DNA (44.1 μM/bp in 10% DMSO/10 mM Tris buffer, pH 8) by $CpW(CO)_3CH_3$ (**10**): lane 1, DNA alone; lane 2, DNA + complex (0.9 mM); lanes 3−7, DNA + complex (0.9 mM) + cysteine (72, 36, 18, 9, and 0.9 mM, respectively); lanes 8−12, DNA + complex (0.9 mM) + TEMPO (72, 36, 18, 9, and 0.9 mM, respectively). Reactions in all lanes except 1 were irradiated as described above.

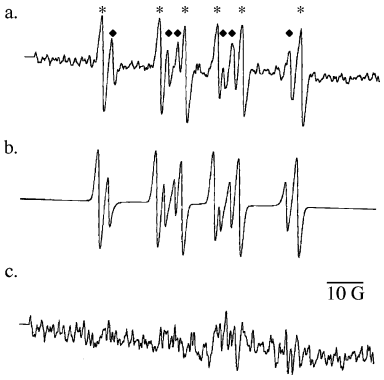

FIGURE 3. EPR spectrum of the photolysis (3 min) reaction mixture of a partially degassed solution of $CpW(CO)_3CH_3$ (**1**, 0.3 mM) and DMPO (20 mM) in 10% DMSO/tris buffer (10 mM, pH 8) at ambient temperature with a medium-pressure mercury lamp: (a) experimental spectrum; (b) simulated spectrum; and (c) difference spectrum (experimental − simulated spectra). All spectra are plotted on the same vertical scale, and the parameters for the experimental spectrum are the following: gain = 2.5×10^4, frequency = 9.434 GHz, power = 50 mW, modulation amplitude = 2 G, modulation frequency = 100 kHz, time constant = 0.250 ms, sweep width = 160 G, sweep time = 240 s. Hyperfine coupling constants obtained by simulation are reported in the text. Peaks marked bu ∗ result from DMPO−CH_3 and those marked by ◆ are assigned to DMPO−CO_2^-.

To investigate the possible participation of methyl radicals in the cleavage process, additional experiments were conducted in which radical scavengers were added to the reaction mixtures before photolysis. When 80 equiv of cysteine, which can function as a general radical trap,[31] were present in the reaction mixture (Figure 2), no cleavage was observed. To discriminate between carbon- and oxygen-centered radicals, cleavage experiments were conducted in the presence of 2,2,6,6-tetramethyl-1-piperdinyloxy (TEMPO), a stable nitroxide that traps

(29) See the Supporting Information.

(30) The source of the H atom has not been determined, but the Cp ring has been implicated: Rausch, M. D.; Gismondi, T. E.; Alt, H. G.; Schwarzle, J. A. *Z. Naturforsch. B* **1977**, *32*, 998−1000.

(31) Huston, P.; Espenson, J. H.; Bakac, A. *Inorg. Chem.* **1992**, *31*, 720−722.

SCHEME 3

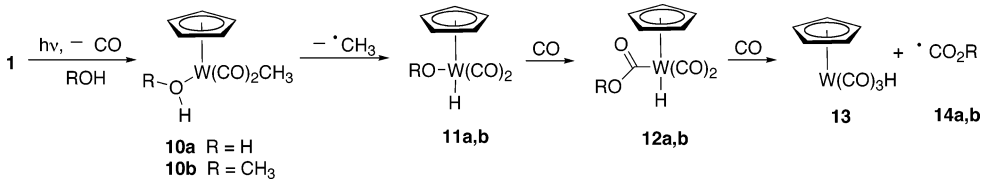

carbon[32] and metal-centered radicals,[33] but not those on oxygen. Thus, when any amount of TEMPO was present, the amount of form II DNA was decreased. While this argues against the involvement of oxygen-centered radicals, it does not preclude the participation of metal-based radicals. However, the contribution of these species to the cleavage is expected to be minimal, because the metal−hydrogen bond strength in similar systems is typically too low[34] to energetically favor hydrogen abstraction from DNA by such radicals. Interestingly, when the photolysis of $[CpW(CO)_3]_2$ (which generates $CpW(CO)_3$ radical but obviously no methyl radical)[35] is conducted in the presence of DNA, a very small amount of cleavage was seen only at concentrations greater than six molecules/base pair and was shown to be inhibited by the presence of TEMPO.[29] Therefore, although an active metal species formed in the reaction cascade may contribute a minor amount, these results implicate methyl radicals or reactive intermediates mechanistically downstream from methyl radicals as the active species giving rise to most of the DNA cleavage resulting from photolysis of **1**.

EPR Studies. In addition to the aforementioned radical-trapping studies, we sought to further probe the involvement of methyl radical in strand scission, using EPR under the aqueous conditions employed in the cleavage studies. Therefore, complex **1** was irradiated in the presence of spin-trap DMPO in 10% DMSO/10 mM Tris buffer, pH 8, resulting in a spectrum (Figure 3a) composed of two radical species. The first of these arises from the trapping of methyl radical by DMPO, a result that is consistent with previous EPR studies of compound **1** in nonaqueous solvents under anaerobic conditions.[19,22] The signals due to the DMPO−methyl adduct exhibit hyperfine coupling constants (a_N = 16.2, a_H = 23.4) in agreement with those previously reported for this species.[36] The methyl radicals also appear not to result from the DMSO cosolvent, since essentially the same pattern was obtained for this species when THF was employed instead of DMSO to solubilize the complex (results not shown).

The second species observed has not been unequivocally identified; however, the hyperfine coupling constants obtained from computer simulation (a_N = 15.6, a_H = 18.6) are identical with those reported for DMPO−CO_2^-.[36] Although the mechanism for the formation of formate radical has not been determined, it is not expected to contribute to strand scission via hydrogen atom abstraction from the backbone of DNA. Such a process is energetically disfavored on the basis of a bond strength argument. Additionally, it has been demonstrated that formate ($HCOO^-$) behaves as a protective agent against hydroxyl radical-induced DNA cleavage[37] by serving as a source of readily abstractable hydrogen atoms to give formate radical ($^{\bullet}COO^-$), which does not cleave DNA.

To elucidate the origins of formate radical produced during the photolysis of $CpW(CO)_3CH_3$ (**1**), this reaction (in methanol instead of water for solubility reasons) was monitored by IR. In these studies, a stretch at 1693 cm^{-1} was identified and assigned to a metal−acyl species, such as compound **12b**,[23,38,39] suggesting the following preliminary mechanism (Scheme 3) for the production of methyl formate radical (**14b**, R = CH_3). Similar behavior would be expected in water, to yield formate radical (**14a**, R = H). Indeed, the 16-electron species formed upon loss of CO from **1** has been reported to coordinate water to produce **10a**;[24] and in other W(II) complexes, the activation of alcohol O−H bonds has been seen.[40,41] Migratory CO insertions such as that occurring in the conversion of **11** to **12** have been observed for tungsten[42] and other[38,43] complexes, as has been the photolytic homolysis of metal−acyl σ-bonds[44] to yield the acyl radical **14** and the precursor to **13**. Alternatively, species such as **12** could be generated by hydroxide/alkoxide attack on a metal-bound carbonyl, as in one step of the $Fe(CO)_5$-mediated water gas shift reaction, although this associative mechanism typically requires more basic conditions and is not observed with $W(CO)_6$ as the catalyst.[45]

These IR studies also provided further support for our assignment of the second species in the EPR spectrum as formate radical. The reaction mixture exhibited a peak at 1733 cm^{-1}, which was assigned to methyl formate, although we have not determined whether it arises from the further reaction of **14b** or via reductive elimination from **12b**.

(32) Connolly, T. J.; Baldoví, M. V.; Mohtath, N.; Scaiano, J. C. *Tetrahedron Lett.* **1996**, *37*, 4919−4922.
(33) Tenhaeff, S. C.; Covert, K. J.; Castellani, M. P.; Grunkemeier, J.; Kunz, C.; Weakley, T. J. R.; Koenig, T.; Tyler, D. R. *Organometallics* **1993**, *12*, 5000−5004.
(34) Tilset, M.; Parker, V. D. *J. Am. Chem. Soc.* **1989**, *111*, 6711−6717.
(35) Bitterwolf, T. E. *Coord. Chem. Rev.* **2001**, *211*, 235−254.
(36) Buettner, G. R. *Free Radical Biol. Med.* **1987**, *3*, 259−303.
(37) Dizdaroglu, M.; Aruoma, O. I.; Halliwell, B. *Biochemistry* **1990**, *29*, 8447−8451.
(38) Wax, M. J.; Bergman, R. B. *J. Am. Chem. Soc.* **1981**, *103*, 7028−7030.
(39) King, R. B.; Bisnette, M. B.; Fronzaglia, A. *J. Organomet. Chem.* **1966**, *5*, 341−356.
(40) Crevier, T. J.; Mayer, J. M. *Inorg. Chim. Acta* **1998**, *270*, 202−206.
(41) Chiu, K. W.; Jones, R. A.; Wilkinson, G.; Galas, A. M. R.; Hursthouse, M. B.; Abdul Malik, K. M. *J. Chem. Soc., Dalton Trans.* **1981**, 1204−1211.
(42) Barnett, K. W.; Beach, D. L.; Gaydos, S. P.; Pollmann, T. G. *J. Organomet. Chem.* **1974**, *69*, 121−130.
(43) Gull, A. M.; Blatnak, J. M.; Kubiak, C. P. *J. Organomet. Chem.* **1999**, *577*, 31−37.
(44) Hudson, A.; Lappert, M. F.; Lednor, P. W.; MacQuitty, J. J.; Nicholson, B. K. *J. Chem. Soc., Dalton Trans.* **1981**, 2159−2163.
(45) King, R. B. *J. Organomet. Chem.* **1999**, *586*, 2−17.

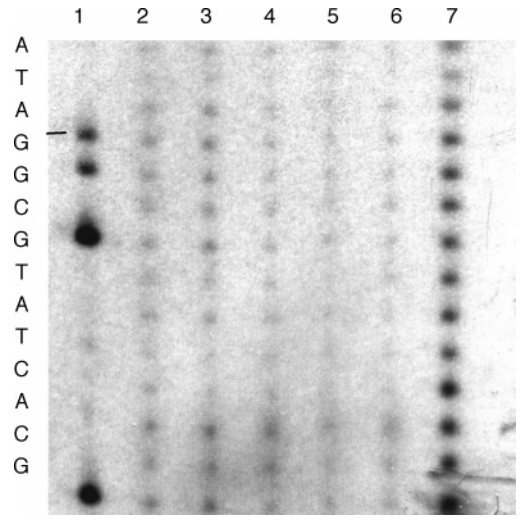

FIGURE 4. Autoradiogram of a portion of a 10% denaturing polyacrylamide gel for photoinduced cleavage of the 3′-^{32}P-end-labeled 514 bp restriction fragment (*Eco*RI/*Rsa*I) of pBR322 DNA/calf thymus DNA (105 μM/bp in 10% DMSO/20 mM Tris buffer, pH 8) by **1**: lane 1, Maxam−Gilbert G reaction; lanes 2 through 6, DNA + complex **1** (2.0, 1.0, 0.5, 0.25, and 0.13 mM, respectively), irradiated; lane 7, DNA + complex (2.0 mM), treated with hot piperidine following photolysis. Reaction mixtures in lanes 2−7 were irradiated with Pyrex-filtered light from a 450-W medium-pressure mercury arc lamp for 20 min.

Interestingly, when complex **1** was photolyzed in the presence of DNA, no DNA-centered radicals were observed by EPR. This result implies either that DNA-centered radicals were not formed or that no single radical species was produced in a high enough concentration to be observed.

Sequence Selectivity of DNA Cleavage. Since the results of EPR and radical scavenging studies with **1** were consistent with the participation of methyl radical at some point in the process that ultimately leads to DNA cleavage under aqueous conditions, a likely mechanism for the direct strand scission observed in the plasmid cleavage assays involved the abstraction of hydrogen atoms from the sugar−phosphate backbone, a process that should be independent of the base sequence of DNA. Therefore, the sequence-selectivity of the photoinduced cleavage of a ^{32}P-end-labeled restriction fragment by $CpW(CO)_3CH_3$ was investigated (Figure 4). As shown in lanes 2 through 6, and as indicated by densitometry of the bands in these lanes, DNA strand scission occurs in a concentration-dependent manner but exhibits no correlation to base sequence. Furthermore, upon treatment with hot piperidine (lane 7), cleavage is enhanced but still shows no sequence variability. This reactivity pattern has been suggested to be typical of cleaving agents that operate via the direct modification of the DNA backbone.[46]

Identification of the DNA-Derived Small Molecule Products of Cleavage. The hypothesis that the mechanism of strand scission by compound **1** involves hydrogen atom abstraction from the sugar−phosphate backbone of DNA is readily tested by examining cleavage reaction mixtures for the known products of these processes. Furthermore, the abstraction of a hydrogen atom from each sugar position gives a unique sugar-derived product, allowing the determination of the position that has been attacked.[47] Abstraction from the 1′-position affords 5-methylene-2-furanone (5-MF),[48,49] and base propenoates result from reaction at the 3′-position.[50] Removal of a 4′-hydrogen leads to the formation of base propenals,[51] and abstraction of a hydrogen from the 5′-position yields furfural (FUR).[48,49] Abstraction from H2′ is not typically observed, presumably because of the low accessibility or reactivity of these hydrogens.[47]

TABLE 1. MALDI-ToF MS Analysis of DNA Cleavage Reaction Mixtures

	rel intensity			
obsd *m/z*	+[a]	−[a]	assignment	calcd *m/z*
165.1	63		C-propenal	165.06
189.2	62		A-propenal	189.07
206.2	25		G-proprenal	206.07
179.9		3	T-propenal	180.06
97.0	104		FUR·H^+	97.03
115.1	175		FUR·H_3O^+	115.04
95.1		90	FUR−H^+	95.01
111.1		18	furoate	111.01

[a] Detection ion mode.

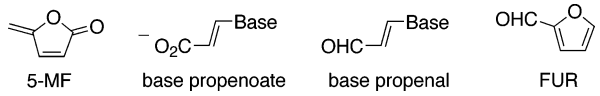

To identify and/or rule out the diagnostic products derived from DNA upon cleavage by **1**, a combination of mass spectrometry and HPLC was employed.[50,52−54,] Thus, after a mixture of **1** and calf thymus DNA was photolyzed, the oligonucleotides were removed by membrane filtration, and the resulting mixture of small molecule products was concentrated prior to further analyses.

In addition to signals that were also observed in the commercial DNA samples, in positive ion mode, MALDI-ToF mass spectrometry of this mixture (Table 1) gave new peaks with *m/z* 165.1, 189.2, and 205.2, which correspond to the C-, A-, and G-propenals with calculated exact masses of 165.06, 189.07, and 206.07, respectively. In addition, two signals at *m/z* 97.0 and 115.1 were observed; the peak at *m/z* 97.0 may be due to either protonated furfural or 5-MF·H^+, both of which have exact masses of 97.03. The other (115.1) could be due to the hydrated protonated form of one of these molecules. In negative ion mode, a signal for T-propenal (exact mass = 180.06) was seen at *m/z* 179.9 and was accompanied by peaks at *m/z* 95.1 and 111.1. The first of these was ascribed again to either furfural or 5-MF (with the mass of the deprotonated form of each equaling

(46) Burrows, C. J.; Muller, J. G. *Chem. Rev.* **1998**, *98*, 1109−1151.

(47) Pogozelski, W. K.; Tullius, T. D. *Chem. Rev.* **1998**, *98*, 1089−1107.

(48) Goldberg, I. H. *Acc. Chem. Res.* **1991**, *24*, 191−198.

(49) Frank, B. L.; Worth, L., Jr.; Christner, D. F.; Kozarich, J. W.; Stubbe, J.; Kappen, L. S.; Goldberg, I. H. *J. Am. Chem. Soc.* **1991**, *113*, 2271−2275.

(50) Sitlani, A.; Long, E. C.; Pyle, A. M.; Barton, J. K. *J. Am. Chem. Soc.* **1992**, *114*, 2302−2312.

(51) Hecht, S. *Acc. Chem. Res.* **1986**, *19*, 383−391.

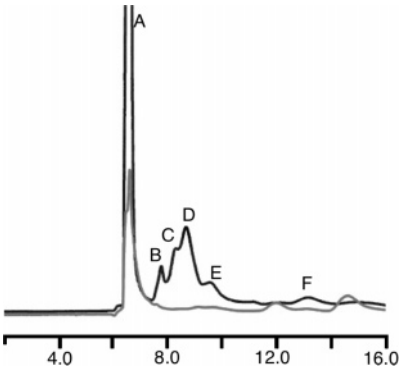

FIGURE 5. HPLC chromatogram of DNA-derived reaction products of calf thymus DNA (8 mM in bp) + complex **1** (2.1 mM) in 10% DMSO/H_2O with irradiation with Pyrex-filtered light from a 450-W medium-pressure mercury arc lamp (black trace) or complex **1** irradiated alone in 10% DMSO/H_2O (gray trace). Peaks in the reaction mixture were assigned by comparison of their retention times to those of authentic samples as follows: A, cytosine + metal complex byproducts; B, hydrated furfural; C, thymine; D, base propenals; E, adenine; F, furfural. Guanine was insoluble under all conditions attempted.

95.01), while the latter signal could not be assigned at this time (but was later determined to be furoate). Therefore, the identification of the base propenals indicated that a hydrogen atom had been removed from the 4′-position of a deoxyribose ring with any base attached; and the possible observation of furfural or 5-MF suggested either H5′ or H1′ abstraction.

The composition of the reaction mixture was examined further by HPLC (Figure 5), for comparison to standard samples of furfural, 5-MF, individual nucleobases, and the base propenoates.[55] While the bases C, T, and A were observed in the cleavage reaction mixture, the lack of solubility of guanine precluded its analysis by this method. These experiments showed that none of the propenoates were produced from the photolysis of **1** in the presence of calf thymus DNA, thus providing additional evidence that H3′ was not abstracted. In addition, no peaks were observed with the retention time found for the 5-MF standard, thus ruling out reaction at the 1′-position and suggesting that the signals at *m/z* 97.0 and 115.1 in the previously described MALDI-ToF studies were due to furfural and its hydrate. The production of furfural was confirmed further by HPLC, which showed a peak that coeluted with a furfural standard, thereby indicating the abstraction of H5′. Additionally, when furfural was added to the DNA cleavage reaction mixture *prior to photolysis*, not only did the peak corresponding to furfural increase, but a second signal at retention time 7.86 min also became larger. Because of this result and because of the previous observation of FUR hydrate by mass spectrometry, the reactivity of furfural under the conditions of $CpW(CO)_3CH_3$ photolysis was studied.

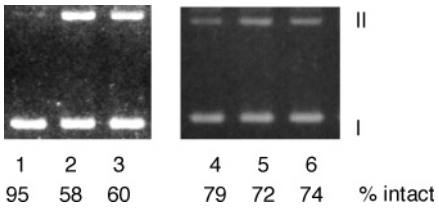

FIGURE 6. Role of oxygen in the $CpW(CO)_3CH_3$-induced cleavage of pBR322 DNA (30 μM/bp in 10% DMSO/20 mM Tris buffer, pH 8): lanes 1 and 4, DNA alone; lanes 2 and 3, DNA + complex (0.72 and 0.36 mM); lanes 5 and 6, DNA + complex, degassed (1.80 and 0.90 mM). Reactions in all lanes except 1 and 4 were irradiated as described above.

Therefore, $CpW(CO)_3CH_3$ was irradiated in the presence of furfural in aqueous methanol, and this reaction mixture was analyzed by FAB-MS, IR, ^{1}H NMR, and ^{13}C NMR. The ^{1}H NMR data suggested that a new compound was formed in the reaction although only approximately a 50% conversion could be achieved. In addition to the signals due to furfural, there were new peaks: a doublet at 7.51 ppm, a multiplet from 6.416 to 6.433 ppm, and a singlet at 5.42 ppm with relative integrations of 1, 2, and 1, respectively. These data and the prior observation of a signal at *m/z* 115.1 suggested the hydration of the aldehyde, which was subsequently confirmed by ^{13}C spectroscopy. Because irradiation of furfural alone in aqueous methanol did not yield any hydrated product, thus indicating the necessity of $CpW(CO)_3CH_3$, it is likely that some coordinatively unsaturated tungsten species functions as a Lewis acid in establishing the equilibrium between **15** and **16** (Scheme 4).

In addition to furfural and its hydrated form, the FAB mass spectrum of the mixture showed a small new peak at *m/z* 111, a value that we had previously observed in the negative ion mode MALDI-ToF MS of the DNA reaction mixtures. These data suggested the oxidation of furfural (**15**) or its hydrate **16** to 2-furoic acid (**17**), a conversion that was confirmed by a new stretch at 1692 cm^{-1} in the IR spectrum of the mixture. Abbreviated mechanisms for these processes are proposed in Scheme 4. Support for the involvement of oxygen in this oxidation was obtained with the finding that no furoic acid was formed when the reaction mixture was degassed by 3 freeze/pump/thaw cycles prior to photolysis.

The Role of Oxygen in Strand Scission. For each of the products shown in Scheme 4, abstraction of hydrogen from the deoxyribose ring is often followed by reaction with oxygen. As a result, the potential role of oxygen was assessed and the results were analyzed by agarose gel electrophoreses (Figure 6), in which the reactions in lanes 5 and 6 were degassed by 3 freeze/pump/thaw cycles prior to irradiation. Although the initial concentration of $CpW(CO)_3CH_3$ in these reactions was much higher than that in aerated samples (lanes 2 and 3), the amount of form II DNA was similar to that observed in the commercial sample (lane 4), indicating that strand scission was almost completely inhibited. This result is consistent with an oxidative cleavage mechanism involving oxygen trapping of the radical formed by hydrogen atom abstraction from the DNA backbone.

(52) Pratviel, G.; Pitié, M.; Bernadou, J.; Meunier, B. *Angew. Chem., Int. Ed. Engl.* **1991**, *30*, 702−704.
(53) Pratviel, G.; Pitié, M.; Bernadou, J.; Meunier, B. *Nucleic Acids Res.* **1991**, *19*, 6283−6288.
(54) Giloni, L.; Takeshita, M.; Johnson, F.; Iden, C.; Grollman, A. P. *J. Biol. Chem.* **1981**, *256*, 8608−8615.
(55) Because the base propenoates (and their conjugate acids) have been only mentioned in the literature, their detailed syntheses and complete characterization are given in the Experimental Section.

SCHEME 4

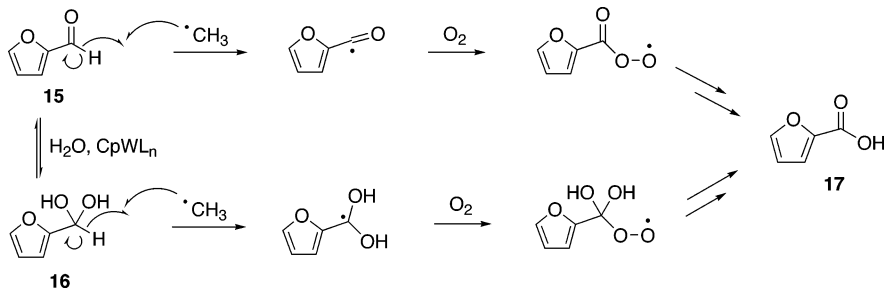

Abasic Site Detection Studies. Another pathway that has been observed in studies with other radical-based agents that abstract hydrogen atoms from deoxyribose units is the creation of abasic sites, many of which result in aldehyde functionality within the backbone of DNA chains.[47] The possible presence of these aldehydes in samples of calf thymus DNA modified by photolysis with varying concentrations of $CpW(CO)_3CH_3$ (**1**) was determined by a colorimetric assay involving the oxidation of 3,3′,5,5′-tetramethylbenzidine by a horseradish peroxidase/streptavidin conjugate bound to the biotin-tagged aldehyde.[56] At concentrations of **1** up to 200 mM, the quantities of abasic sites were equivalent to those seen in control samples of DNA (i.e., treated with **1** but not irradiated, irradiated without **1**, and without irradiation or **1**). This result indicated that no significant amount of additional abasic sites was created upon reaction of DNA with the photolysis products of **1**.

Detection of Modified Nucleobases. In addition to hydrogen atom abstraction from deoxyribose rings, another possible reaction of methyl radical with DNA is the alkylation of the bases, which has been shown to vary with respect to both nucleobase and position depending on pH.[57] Since such modified bases would remain incorporated in the DNA, they would not be observed in any of the previously described experiments. Therefore, following the photolysis of a mixture of **1** and calf thymus DNA, the reaction mixture was hydrolyzed with formic acid at 140 °C to cleave the glycosidic bonds between bases and sugars, removing both the functionalized and unreacted bases from backbone but otherwise leaving them intact. These modified samples were then analyzed by MALDI-ToF MS, the results of which were compared to those obtained from an unmodified but hydrolyzed portion of commercial DNA (Table 2). In both samples, signals at *m/z* 112.5, 127.4, 136.4, and 152.7 were observed, corresponding to the protonated forms of C, T, A, and G, respectively. In the sample that had been treated with $CpW(CO)_3CH_3$ and photolyzed, additional peaks were seen at *m/z* 126.4, 141.3, 150.5, and 166.5, corresponding to methylated, protonated C, T, A, and G, respectively. Clearly, with the relative intensities of the signals in the MS of the unmodified sample being inequivalent for paired bases (G vs C or A vs T), these particular experiments must not reflect the base composition of the DNA.[58] Therefore, no conclusions can be drawn from the peak intensities in either sample. Thus, the methyl radical produced via the photolysis of $CpW(CO)_3CH_3$ reacts with all four bases to give methylated products, and none of these functionalized bases are released under the DNA cleavage conditions.

TABLE 2. MALDI-ToF MS Detection of Modified DNA Bases

	rel intensity			
obsd *m/z*	unmodified[a]	modified[b]	assignment	calcd *m/z*
112.5	32.0	21.2	C·H$^+$	112.06
125.8	0	19.5	MeC·H$^+$	126.04
126.5	14.8	13.4	T·H$^+$	127.06
136.4	38.5	11.7	A·H$^+$	136.07
141.3	0	18.0	MeT·H$^+$	141.07
150.5	0	7.2	MeA·H$^+$	150.08
152.5	14.7	4.9	G·H$^+$	153.07
166.5	0	4.0	MeG·H$^+$	167.08

[a] Not treated. [b] Treated with **1**.

Discussion

Altogether, the evidence suggests that the mechanism of DNA cleavage via the photolysis of $CpW(CO)_3CH_3$ (**1**) involves the radical-mediated oxidative modification of the deoxyribose moieties, shown in an abbreviated form in Scheme 5. The production and involvement of methyl radical were indicated by two sets of experiments: (1) EPR studies, in which only DMPO-trapped methyl and formate radical were observed, and (2) the inhibition of plasmid DNA strand scission by the radical scavenger TEMPO, which selectively traps carbon- and metal-centered radicals. However, metal-centered radicals are most likely not responsible for DNA cleavage by hydrogen atom abstraction, as predicted by the low metal hydride bond strength of such species [65 kcal mol^{-1} for $CpW(CO)_3H$[34]] and as shown by the lack of strand scission by photogenerated $CpW(CO)_3$ radical (although the production of this species may not be relevant in the photochemical reactions of **1**). Nor does formate radical, another side product of the photolysis of **1**, contribute to DNA cleavage, for the reasons discussed previously.

The photogenerated methyl radical, on the other hand, could lead to strand scission via two possible routes, neither of which can be ruled out by the experiments reported herein. Thus, methyl radical could next react with DNA directly by abstracting a hydrogen atom from a deoxyribose ring, in a manner analogous to the reaction

(56) Ide, H.; Akamatsu, K.; Kimura, Y.; Michiue, K.; Makino, K.; Asaeda, A.; Takamori, Y.; Kubo, K. *Biochemistry* **1993**, *32*, 8276−8283.
(57) Hix, S.; Da Silva, M.; Augusto, O. *Free Radical Biol. Med.* **1995**, *19*, 293−301. Augusto, O. *Free Radical Biol. Med.* **1993**, *15*, 329−336. Zady, M. F.; Wong, J. L. *J. Org. Chem.* **1983**, *45*, 2373−2377.
(58) Kuo, K. C.; McCune, R. A.; Gehrke, C. W. *Nucleic Acids Res.* **1980**, *8*, 4763−4776.

of methyl radical with THF (Scheme 2), or it can react with oxygen to produce the methylperoxyl radical **18**. While our studies of the photolysis of **1** in THF-d_8 as a simple DNA mimic gave the product CH_3D resulting from deuterium abstraction by methyl radical (Scheme 2), this result may not reflect the pathway occurring in the DNA cleavage studies, in which the concentration of DNA is lower and the concentration of oxygen higher. On the basis of the rate constants for hydrogen atom abstraction by alkyl radicals (e.g., $k = 6.0 \times 10^3$ M^{-1} s^{-1} at 25 °C for the reaction of a primary radical with H_α of THF[59]) and for the reaction of methyl radical with oxygen (4.7×10^9 M^{-1} s^{-1}),[60] DNA concentrations of 30 μm/bp, and the known solubility of oxygen in water (3.16 cm^3/100 mL), we can estimate that the methyl radical reacts with oxygen about 10^6 times faster than it abstracts a hydrogen from DNA in this system, assuming no precomplexation of **1** with DNA prior to photolysis.

However, ethidium bromide displacement assays[61] show that **1** does bind weakly (with an apparent binding constant $K_{app} = 5.44 \times 10^4$ M^{-1}) to DNA in nonirradiated samples. This interaction effectively increases the rate of the reaction of methyl radical with DNA, an expectation that is confirmed in a qualitative sense by the identification of methylated nucleobases by MS of the irradiated reaction mixtures of **1** with DNA. Nevertheless, it is difficult to predict in a quantitative manner how much the binding of **1** to DNA affects the partitioning between DNA and oxygen in the reactions of methyl radical. Furthermore, because both pathways involve methyl radical, both would be inhibited by the carbon radical scavenger TEMPO, as was observed (Figure 2).

It has been asserted that the product of the latter reaction, methylperoxyl radical (**18**), is a poor hydrogen atom abstractor that preferentially dimerizes to give the unstable tetraoxide **19**,[62] an argument that is presumably based on the relative rate constants for similar processes. For example, rate constants on the order of 10^7 M^{-1} s^{-1} are typical for the dimerization of primary alkylperoxyl radicals,[63] while those for hydrogen abstraction by *tert*-butylperoxyl radical range from 10^{-2} M^{-1} s^{-1} for allylic or benzylic hydrogens[63] to 10^3 M^{-1} s^{-1} for phenol.[59] Therefore, with such values, for hydrogen abstraction from deoxyribose to occur at a faster rate than dimerization in our system, the concentration of methylperoxyl radical must be below 0.03 nM (using the higher value, $k = 10^3$ M^{-1} s^{-1}, for hydrogen abstraction). Considering the initial concentration of **1** necessary for strand scission (at least 45 μM), the reported yield (95%) for the conversion of **1** to $[CpW(CO)_3]_2$ (which is thought to be coupled to methyl radical production),[23] and the efficiency of the reaction of methyl radical with oxygen, the concentration of **18** could be high enough for the production of **19** to dominate, unless it is reduced by the competitive reaction of methyl radical directly with DNA.

Such dimerization of methylperoxy radical, although a termination process, may not preclude DNA cleavage. For dialkyltetroxides with primary alkyl groups, the *thermal* decomposition pathway has been shown to give formaldehyde, methanol, and oxygen, presumably via a concerted reaction involving a six-membered cyclic transition state.[63] Although none of these products cleave DNA, the *photolytic* reaction of the tetroxide **19** could yield oxygen and dimethylperoxide **20**, by analogy to a similar reaction of di-*tert*-butyltetroxide.[63] From here, the photolytic homolysis of the oxygen−oxygen bond in species such as **20** is well established; and alkoxyl radicals such as **21** are known to be very efficient hydrogen atom abstractors.[59] The fact that no peaks corresponding to the DMPO adduct of either **18** or **21**[64] were observed via EPR (Figure 3) can be ascribed to the fact that this spectrum was obtained with a partially degassed sample.[65] The next step of the cleavage process involves the abstraction of a hydrogen atom from the deoxyribose ring of the backbone of DNA. This hypothesis is consistent with the lack of sequence-selectivity observed in strand scission (Figure 4) and is further supported by the identification of the deoxyribose-derived products, furfural (**23**) and the base propenals **22** (Table 1). These products also indicate that hydrogen atom abstraction occurs at the 5′- and the 4′-positions of the sugar, and the mechanisms shown in Scheme 5 for these processes are based on those proposed for DNA cleavage by neocarzinostatin[48,49] and bleomycin-Fe(II),[51] respectively. Other small molecule side products of reaction at 5′ are the nucleobases, which were detected by HPLC (Figure 5), a finding that is consistent with a previous report of DNA cleavage involving methyl radical.[16]

Unfortunately, the identification of these products provides no information on whether the active abstracting species is methyl or methoxyl radical (**21**); and the mechanism of DNA strand scission by methoxyl radical with DNA has been mentioned but not yet determined[66] for comparison to our results. Other alkoxyl radicals have been shown to cleave DNA;[67] but their cleavage mechanisms are also not known, except in the case of *tert*-butoxyl radical, which produces primarily 8-oxoguanine.[68] Interestingly, this oxidized base was not observed in any reaction mixtures resulting from the photolysis of **1** with DNA. This result, coupled with the previously discussed observation of methylated bases, suggests that the reaction of methyl radical directly with DNA (instead of oxygen first) is a significant pathway for DNA damage, if not the exclusive one.

(59) Fossey, J.; Lefort, D.; Sorba, J. *Free Radicals in Organic Chemistry*; John Wiley and Sons: New York, 1995.
(60) Neta, P.; Huie, R. E.; Ross, A. B. *J. Phys. Chem. Ref. Data* **1990**, *19*, 413−513.
(61) Morgan, A. R.; Lee, J. S.; Pulleyblank, D. F.; Murray, N. L.; Evans, D. H. *Nucleic Acids Res.* **1979**, *7*, 547−569.
(62) Sawyer, D. T.; Kang, C.; Llobet, A.; Redman, C. *J. Am. Chem. Soc.* **1993**, *115*, 5817−5818.
(63) Sheldon, R. A.; Kochi, J. K. *Metal-Catalyzed Oxidations of Organic Compounds*; Academic: New York, 1981.
(64) Interestingly, numerous researchers have reported the DMPO adduct of **18**,[36] but it now appears that this species is probably DMPO·OCH_3, derived from **21**: Dikalov, S. I.; Mason, R. P. *Free Radical Biol. Med.* **1999**, *27*, 864−872.
(65) Unfortunately, the EPR spectrum of a nondegassed sample was too complex for the unambiguous assignment of these species.
(66) Gould, I. R., Arizona State University, personal communication, 2005.
(67) Adam, W.; Hartung, J.; Okamoto, H.; Marquardt, S.; Nau, W. M.; Pischel, U.; Saha-Möller, C. R.; Spehar, K. *J. Org. Chem.* **2002**, *67*, 6041−6049. Adam, W.; Arnold, M. A.; Grimm, G. N.; Saha-Moller, C. R.; Dall'Acqua, F.; Miolo, G.; Vedaldi, D. *Photochem. Photobiol.* **1998**, *68*, 511−518. Adam, W.; Grimm, G. N.; Saha-Moller, C. R. *Free Radical Biol. Med.* **1997**, *24*, 234−238.
(68) Mahler, H.-C.; Schulz, I.; Adam, W.; Grimm, G. N.; Saha-Möller, C. R.; Epe, B. *Mutat. Res.* **2001**, *461*, 289−299.

SCHEME 5

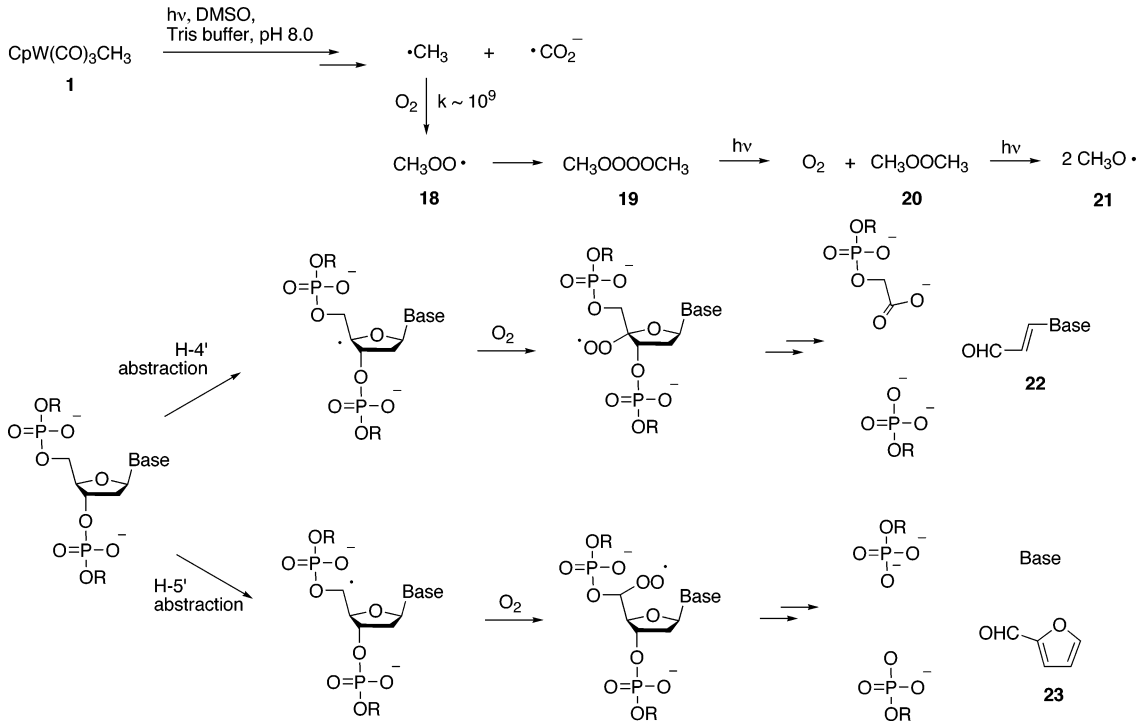

SCHEME 6

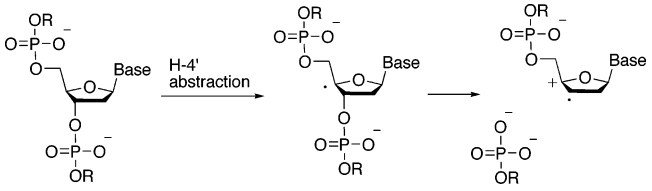

In any case, hydrogen atom abstraction from the deoxyribose moiety is followed by the reaction of the sugar-based radicals with molecular oxygen, a proposal that is consistent with the finding that plasmid DNA cleavage is reduced significantly when oxygen is removed from the reaction mixture prior to photolysis (Figure 6). The observation that some strand scission was still observed in these experiments may be the result of the incomplete degassing of the solution or of the fact that oxygen is not required in an alternate mechanism originating with hydrogen abstraction at 4′ (Scheme 6).[69] At various points in these mechanisms, side products are produced, although none appear to contribute to frank strand scission. In the photolysis of **1**, formate radical is formed but does not damage DNA, as discussed previously. In the subsequent reaction of methyl radical with DNA, strand scission by hydrogen atom abstraction is accompanied by base methylation, although no methylated bases are released. Additionally, the furfural that is produced by H5′ abstraction reacts further under the reaction conditions to yield furfural hydrate and a small amount of furoic acid.

Finally, a number of processes have been ruled out in these experiments. The DNA-derived products from the abstraction of hydrogen from positions other than 4′ and 5′ (5-methylenefuranone from 1′ hydrogen atom abstraction or the base propenoates from reaction at 3′) were not seen; and this result is consistent with the combination of the decreased accessibility of these hydrogens[47] and the larger size of methyl vs hydroxyl radical. Another mechanism involving the oxidation of nucleobases was also a possibility; however, no evidence for this pathway was seen. Not only does base oxidation lead to only minimal amounts of strand scission in plasmid assays, but it also leads to the preferential cleavage at G residues,[46] observations which are inconsistent with our results (Figure 4). Furthermore, none of the products typical of guanine oxidation (for example, FAPy-G or 8-oxo-G) were detected in any reaction mixtures of **1** with DNA.

Experimental Procedures

Plasmid Relaxation Assays. A DMSO solution was made of the compound of interest and serial dilutions were made. The appropriate DMSO solution was added to a 1.5 mL plastic centrifuge tube containing 9 times the volume of a solution containing either 33.3 or 66.6 μM/bp DNA (pBR322) in 20 mM tris-HCl reaction buffer, pH 8 (final concentration = 30.0 or 60.0 μM/bp). The tubes were then strapped to the outside of a water-jacketed reaction vessel for photolysis with a 450-W medium-pressure mercury arc lamp with a Pyrex filter. In all photolyses, room-temperature water flowed through the jacket to keep the reaction mixtures at ambient temperature; and all reaction tubes were 5 cm from the center of the lamp. After 20 min of irradiation, 5 μL of loading buffer was added to each sample and the contents of the tube were loaded onto a 1% agarose gel and electrophoresed for 12 h at 30 V. The gel was then stained in a dilute solution of ethidium bromide (~0.5 μg/mL) for 10 min and then destained with water. The DNA was visualized with UV light and photographed with a Polaroid DS34 camera with black and white Polaroid 667 film.

Cleavage with $CpW(CO)_3CH_3$ (1) and High-Resolution Gel of Electrophoresis of Restriction Fragments. Reac-

(69) Giese, B.; Beyrich-Graf, X.; Erdmann, P.; Petretta, M.; Schwitter, U. *Chem. Biol.* **1995**, *2*, 367−375.

tions were carried out in 1.5 mL plastic microcentrifuge tubes. A DMSO solution (2 μL) of **1** was added to 18 mL of a solution containing 3′-^{32}P-labeled restriction fragment (50 000 cpm) and carrier calf thymus DNA (118 μM bp) in tris acetate buffer (pH 8). The microcentrifuge tubes were strapped to the outside of a water-cooled Pyrex photolysis reactor and irradiated with light from a 450-W medium-pressure mercury arc lamp for 20 min. After the photolysis, the DNA was precipitated by adding 2 μL of NaOAc (3 M, pH 5) and 50 μL of absolute ethanol. The samples were cooled at −20 °C for 1 h and then centrifuged at 4 °C at 13 000 rpm for 10 min. The supernatant was removed and the samples were resuspended in 5 μL of formamide loading buffer. Each sample was heated at 95 °C for 3 min and immediately cooled on ice for 1 min prior to loading onto a 10% denaturing polyacrylamide gel (1:19 cross-linking, 7 M urea) along with the Maxam-Gilbert G sequencing reaction and footprinting assays. The samples were electrophoresed at 55 W and 55 °C for 1.5 h. After electrophoresis, the gel was blotted with a positively charged membrane for 20 min. After cross-linking each section of the membrane for 3 min with UV light, the membrane was exposed to X-ray film with an intensifying screen for 72 h at −40 °C.

EPR Spectroscopy. A DMPO stock solution (0.3 M) was made as previously described[70] to remove paramagnetic impurities, and its final concentration was determined by UV−visible spectroscopy. EPR samples were prepared by mixing this stock solution with a solution of **1** (0.3 mM in 10% DMSO/Tris buffer, 10 mM, pH 8.0). The sample was then transferred to a quartz EPR flat cell and was photolyzed for 3 min as previously described, and EPR measurements were accomplished immediately thereafter. Hyperfine coupling constants (a_H and a_N) were determined by computer simulation[71] of the observed spectrum, after calibration of the instrument with 2,2-diphenyl-1-picrylhydrazyl (DPPH) and Fremy's salt. The simulations were run without constraining the hyperfine coupling constants, *g*-values, line widths, and line shape.

Analysis of DNA-Derived Cleavage Products from Photolysis Reactions with $CpW(CO)_3CH_3$ (1). To a 450-μL solution of calf thymus DNA (4.4 mg/mL in distilled deionized H_2O) was added 50 μL of a solution of compound **1** (21.7 mM in DMSO). This mixture was irradiated for 20 min through a Pyrex filter, using a 450-W medium-pressure mercury arc lamp. The solution was then transferred to Microcon-3 tubes and centrifuged at 13 500 rpm for 45 min. The filtrate was then concentrated with a centrivap concentrator and stored in the freezer for further use.

HPLC Analysis of Cleavage Products. Two photolysis reaction mixtures were combined and analyzed on a Bondapack 10μ C_{18} reverse phase column eluted with 90/10 0.1 M triethylammonium acetate/acetonitrile at 0.5 mL/min, with UV detection at $\lambda = 254$ nm.

MALDI-ToF Analysis of Cleavage Products. Two photolysis reaction mixtures were combined, concentrated, and loaded on a DIOS strip. The strip was placed in a vacuum desiccator until dry. The DIOS strip was then loaded into the MALDI-ToF spectrometer for analysis. Linear negative and linear positive modes of operation were utilized. Mass acquisition range: 50−300 Da; 200 laser shots/spectrum.

Detection of Base Modifications. To a 105 μL solution of calf thymus DNA (1.1 mg/mL in distilled deionized H_2O) was added 11.7 μL of a solution of compound **1** (21.0 mM in DMSO). This mixture was irradiated for 20 min through a Pyrex filter, using a 450-W medium-pressure mercury arc lamp. The mixture was then hydrolyzed with 0.5 mL of 60% (v/v) formic acid in a sealed tube at 140 °C for 30 min. This mixture was then analyzed by MALDI-ToF-MS as stated above. In addition, a 105 μL solution of calf thymus DNA (1.1 mg/mL in distilled deionized H_2O) was hydrolyzed with 0.5 mL of 60% (v/v) formic acid in a sealed tube at 140 °C for 30 min. The mixture was then analyzed by MALDI-ToF-MS as stated above to serve as a control.

Furfural Control Experiments. To 900 μL of a 1.14 M solution of furfural in CD_3OD was added 100 μL of a 21.7 mM $CpW(CO)_3CH_3$ solution in DMSO. The mixture was irradiated for 20 min through a Pyrex filter, using a 450-W medium-pressure mercury arc lamp. The mixture was filtered through Celite and analyzed by NMR, FAB-MS, and IR. FT-IR: 1692.40 cm^{-1} (C=O, 2-furoic acid), 1675.35 cm^{-1} (C=O, furfural). ^{1}H NMR (CD_3OD): δ 6.412−6.431 (m, 2H), 6.705−6.723 (m, 1 H), 7.432 (d, J = 3.6 Hz, 1H), 7.510 (br s, 1H), 7.904 (br s, 1H). ^{13}C NMR (CD_3OD): δ 99.313, 109.645, 111.255, 113.965, 123.568, 143.903, 150.232, 152.571, 154.580, 179.702. FAB-MS: *m/z* 111.

Abasic Site Detection. To each of a series of 5.0 μL solutions of calf thymus DNA (1.1 mg/mL in distilled deionized H_2O) was added 2.2 μL of a solution of compound **1** in DMSO to achieve the final concentrations of **1** of 200, 100, 50, 25, 12.5, 6.3, and 3.1 μM. Each sample was prepared and tested in duplicate, and controls were prepared with the aforementioned DNA solution and DMSO without **1**. These mixtures were irradiated for 20 min through a Pyrex filter, using a 450-W medium-pressure mercury arc lamp. The number of abasic sites in each sample was then determined with a DNA Damage Quantification Kit from Dojindo Molecular Technologies. The calibration curve and results from experiments with $CpW(CO)_3CH_3$ are given in the Supporting Information.

Acknowledgment. We thank William R. Nadler, Angela D. Kerekes, and Tricia L. Scott for their preliminary experimental contributions to this work. We acknowledge the American Cancer Society, Emory University, and West Virginia University for support of this work, as well as shared instrumentation at Emory provided by grants from the NIH and NSF.

Supporting Information Available: Quantitation data for all gels, agarose gel analysis for solvent studies and control experiments with $[CpW(CO)_3]_2$, detailed experimental procedures for the preparation of the base propenoates, and data for abasic site quantitation experiments. This material is available free of charge via the Internet at http://pubs.acs.org.

JO050338H

(70) Floyd, R. A.; Lewis, C. A.; Wong, P. K. *Methods Enzymol.* **1984**, *105*, 231−237.

(71) EPR simulations were carried out with the WINSIM implementation of PEST, which is available form NIEHS (http://EPR.niehs.nih.gov/pest.html).